Applied Catalysis B: Environmental 99 (2010) 163–169

Contents lists available at ScienceDirect

Applied Catalysis B: Environmental

journal homepage: www.elsevier.com/locate/apcatb

Cobalt exchanged zeolites for heterogeneous catalytic oxidation of phenol in the presence of peroxymonosulphate

Pradeep Shukla [a], Shaobin Wang [a,*], Kailash Singh [b], H.M. Ang [a], Moses O. Tadé [a]

[a] Department of Chemical Engineering and CRC for Contamination Assessment and Remediation of the Environment (CRC-CARE), Curtin University of Technology, GPO Box U1987, Perth, WA 6845, Australia
[b] Department of Chemical Engineering, Malaviya National Institute of Technology, Jaipur 302017, India

ARTICLE INFO

Article history:
Received 17 March 2010
Received in revised form 25 May 2010
Accepted 8 June 2010
Available online 12 June 2010

Keywords:
Advanced oxidation
Wastewater treatment
Phenol
Co catalyst
Sulphate radical

ABSTRACT

Several cobalt ion-exchanged zeolite catalysts based on ZSM-5, zeolite-A, and zeolite-X were prepared and tested for heterogeneous oxidation of phenol in the presence of various oxidants such as H_2O_2, persulphate, and peroxymonosulphate. It is found that Co-ZSM-5 is highly effective in heterogeneous activation of peroxymonosulphate to produce sulphate radicals but exhibits low activity for the activation of H_2O_2 and persulphate for organic oxidation in water. Co-zeolite-A and Co-zeolite-X show much faster reaction rate in homogeneous activation of peroxymonosulphate due to decomposition of the catalysts and leaching of Co ions into aqueous solution. Co-ZSM-5 also presents stable performance in heterogeneous activation of peroxymonosulphate for phenol degradation. The phenol degradation depends on catalyst loading, phenol concentration, oxidant concentration and temperature. Kinetic studies indicate that phenol degradation follows zero-order kinetics with an activated energy of 69.7 kJ/mol.

1. Introduction

The rising problem of water pollution has posed a big challenge to both industry and society in terms of their economical growth and sustainability. Pollutants such as phenol and chlorophenols arising from refineries are highly toxic and comparatively more refractory to natural degradation thereby causing a potential threat to the land and surface water system even if discharged in a minute quantity. Experience from many developed nations has also suggested the danger to the underground water contamination due to the leaching of the pollutants, thus making it imperative to reduce the pollutant concentration to a safer limit before discharging. Due to the persistent nature of such pollutants, conventional techniques based on primary and secondary waste treatment systems such as activated sludge treatment fail to achieve the desired pollutant destruction. Tertiary treatment techniques such as advanced oxidation processes have been proven to be quite effective for complete destruction of phenolic wastes. Techniques such as wet air oxidation (WAO) have been successfully applied for the treatment of an array of pollutants, but it is highly energy consuming, requiring high temperature and pressure. The economics of WAO process is generally dependent on the extent of chemical oxidation demand (COD), and this technique is well off only for the wastewater with COD from 20 to 200 mg/l; further higher content of COD would require incineration [1]. In order to enhance the generation of active radicals for the oxidation at normal temperature and pressure conditions, several external activating agents such as ozone, UV radiation and chemical oxidants have been used and tested [2–5]. Ozonation, in spite of being quite efficient, also requires high energy source. Among others, chemical oxidation of organic pollutants in the presence of a catalyst has aroused a greater interest due to lower energy requirements and faster reaction rate.

Catalytic oxidation of organic pollutants using hydrogen peroxide to generate active hydroxyl radical has been extensively used for phenolic contaminant degradation. Iron has been found to be highly effective in breaking the peroxide to generate active hydroxyl radicals, which is highly active for oxidising the organic contaminants [2]. Although, the Fenton oxidation is one of the most popular advanced oxidation technique and is used in several industrial applications for the treatment of industrial discharged streams, it faces several limitations such as requirement of low pH, formation of precipitate, limited total organic carbon removal, and quenching of hydroxyl radical by the carbonate species present in the system. In the last few years, there has been significant research in an alternative technology to the Fenton reagent for degradation of various organic contaminants. The important oxidation process involves the utilisation of peroxymonosulphate based oxidant in the presence of cobalt ions to generate active sulphate and hydroxyl radicals [6–10].

* Corresponding author. Tel.: +61 8 9266 3776; fax: +61 8 9266 2681.
E-mail addresses: Shaobin.wang@curtin.edu.au, wangshao@vesta.curtin.edu.au (S. Wang).

0926-3373/$ – see front matter © 2010 Elsevier B.V. All rights reserved.
doi:10.1016/j.apcatb.2010.06.013

Similar to hydrogen peroxide, peroxymonosulphate has been proposed as an alternative oxidant. In the presence of cobalt catalyst, the peroxymonosulphate breaks up to generate active sulphate radical which in turn helps in oxidising pollutants as shown below [6,7]:

$$Co^{2+} + HSO_5^- \rightarrow Co^{3+} + SO_4^{\bullet -} + OH^- \quad (1)$$

$$SO_4^{\bullet -} + H_2O \rightarrow SO_4^{2-} + OH^{\bullet} + H^+ \quad (2)$$

$$SO_4^{\bullet -} + C_6H_5OH \rightarrow C_6H_5OH - SO_4^{\bullet -} \xrightarrow{-SO_4^{2-}} C_6H_5OH^{\bullet +} \xrightarrow{\text{several steps}} CO_2 + H_2O \quad (3)$$

Sulphate radical has a higher oxidation potential [2.5–3.1 eV] as compared to the hydroxyl radical [1.7 eV], thereby promising to be an efficient oxidant. However, the oxidation reaction using cobalt and peroxymonosulphate under homogeneous system has profound disadvantage in terms of cobalt loss. The loss of cobalt in discharged stream renders its toxic as cobalt is recognised as a priority metal pollutant. It leads to several health problems such as asthma, pneumonia and other lung problems [11]. In order to make this technology commercially feasible, it is essential to prevent the loss of cobalt species. In the past few years, several attempts have been made in developing supported cobalt catalysts for heterogeneous oxidation systems. Dionysiou et al. [12] have reported the application of cobalt oxide for the treatment of dichlorophenol. Although it was observed that heterogeneous cobalt oxide (Co_2O_3) was capable of activating peroxymonosulphate, a considerable leaching of cobalt was observed. Further attempts to immobilise cobalt onto various supports such as SiO_2, Al_2O_3 and TiO_2 have shown promising outcomes [4,13]. In all the cases, various cobalt precursors were loaded onto the supports by wet impregnation and the cobalt leaching could not be completely prevented, rendering the catalyst unusable after twice or more uses.

Various types of zeolites have been used as adsorbents, catalyst supports, and catalysts. Co-zeolite has been successfully synthesised in the past by various techniques such as ion exchange or impregnation [14] and used successfully for various applications such as Fischer-Tropse reaction [15], epoxidation of styrene [16], and adsorption of CO_2 [17]. It is believed that Co ion by ion exchange can be retaining on the surface and the cobalt species can also maintain at cobalt oxidation state [14,18,19]. However, Co-zeolite has not been used as a heterogeneous catalyst in generation of sulphate radicals for organic oxidation in aqueous solution. In this study, three different types of zeolites (A, X and ZSM-5) were exchanged with cobalt and the reaction kinetics for the oxidation of phenol with sulphate radical were studied.

Zeolite-A has a cubic structure and is distinguished by Si/Al ratio of 1 which provides the maximum amount of exchangeable cation per mole of the sample. In zeolite-A, cobalt ion is generally located in the central sodalite cage or on the surface of unit cell [20]. Zeolite-X belongs to Faujasite type having the Si/Al ratio of 1.25, thus having lesser number of exchangeable cations per mole as compared to zeolite-A. In this zeolite, cobalt ion is generally located at 5 different sites in the unit cell [21]. In contrast to zeolite-A and -X wherein the cobalt ion is generally in the exchangeable form, ZSM-5 type of zeolite docks the cobalt in two different forms, i.e. Co^{2+} ions in the exchangeable form or an oxide form as CoO clusters. The CoO or the oxide like structure is formed due to the interaction of Co^{2+} with the intra-structural water molecules [22].

2. Experimental

2.1. Materials

Powdered zeolites A, X, and ZSM-5 were supplied by the Zeolite and Allied Products, Mumbai, India. Cobalt chloride ($CoCl_2{\cdot}6H_2O$) purchased from Aldrich was used as a cobalt precursor for ion exchange. Peroxymonosulphate (PMS), which is available as a triple salt of sulphate commercially known as oxone ($2KHSO_5{\cdot}KHSO_4{\cdot}K_2SO_4$), was obtained from Aldrich and used as an oxidant. Pure methanol was used as a quenching reagent to stop the reaction in the sample bottle before high performance liquid chromatography (HPLC) analysis and sodium nitrile was used for quenching the reaction before the total organic carbon (TOC) analysis. Ethanol and tert-butanol obtained from Aldrich were used for radical quench tests. Phenol from Aldrich was used to prepare a stock solution at 5000 ppm. H_2O_2 (30 wt%) and potassium persulphate were also obtained from Aldrich.

2.2. Cobalt ion exchange on zeolites

Cobalt ion was loaded in zeolite samples following a conventional ion-exchange technique. The concentration of cobalt ion in the solution for ion exchange was almost twice the maximum moles of cobalt capable of being exchanged into the zeolites. In brief a fixed amount of zeolite samples were added to cobalt chloride solution in solid to liquid ratio of 1:60 and stirred under reflux condition for 6 h at 75 °C. The solution was filtered and washed with warm distilled water until free from chloride ions. The procedure was repeated 3 times to ensure the maximum exchange of the ions. Finally the samples were dried at 75 °C and stored in a desiccator until use.

2.3. Characterisation of catalysts

The crystallinity of various zeolite samples was studied using X-ray diffraction (XRD). The spectra were obtained on a Simens XRD instrument, using filtered Cu Kα radiation with accelerating voltage of 40 kV, current of 30 mA and scanned at 2θ from 5° to 70°. The crystallinity of the samples was calculated based on the intensity ratio of five major peaks as per Eq. (4). The XRD pattern of sodium exchanged zeolite was used as a reference:

$$\%\text{crystallinity} = \frac{\text{sum of peak intensities of sample}}{\text{sum of peak intensities of reference}} \times 100 \quad (4)$$

The texture and morphology of the prepared samples were observed using scanning electron microscopy (SEM). For analysis, the samples were sputtered gold coated in order to make the sample conducting and to easily distribute the charge. The analysis was done mostly with a secondary electron detector in order to focus on the particle's surface features. UV–vis diffuse reflectance spectroscopic (DRS) studies were carried out using a Jasco V-570 equipped with an integrating sphere at the room temperature in air. $BaSO_4$ was used as the reference material. The spectra were recorded in the wavelength range of 200–800 nm.

2.4. Kinetic study of phenol oxidation

The catalytic oxidation of phenol was carried out in a 500 ml reactor filled with phenol solution of varying concentrations. The reactor was partially immersed in a water bath fitted with a temperature controller. The reaction mixture was stirred with a plastic coated stirrer to maintain homogeneous solution. Before the reaction, a known amount of oxidant peroxymonosulphate was added to the mixture and was allowed to dissolve. Later a fixed quantity of

catalyst (Co-zeolite) depending on the predefined reaction parameter was added to start the reaction. The reaction was carried out for 6 h, and during a fixed interval, 0.5 ml of sample was withdrawn using a syringe filter into a HPLC vial to which 0.5 ml high purity methanol was added to quench the reaction. A few other tests were carried out with different oxidants, H_2O_2 and peroxydisulphate (PDS).

The phenol concentration was analysed using a Varian HPLC with a UV detector at the wavelength of 270 nm. The C-18 column was used to separate the organics while the mobile phase consisting of 30% CH_3CN and 70% water was used as the transport medium. For a few selected experiments, total organic content was also determined using a Shimadzu TOC-5000 CE analyser. For the measurement of TOC, 5 ml sample was extracted at an interval of 1 h and quenched with 5 ml of 3 M sodium nitrile solution and then analysed on the TOC analyser. The concentration of peroxymonosulphate was analysed by a titration method. In brief, 5 ml of reaction mixture containing peroxymonosulphate was mixed with 2 g of KI and was shaken vigorously. After that, 0.2 g of Vitrx indicator was added and left for 15 min. Finally, 1 ml of glacial acetic acid was mixed into the solution and shaken well. The resultant mixture was titrated with sodium thiosulphate. Lastly the radical quenching studies were also carried out to determine the type of active radical formed in the reaction. Two different kinds of quenching reagent, *viz.* ethanol and tertiary butanol, were used for the study.

2.5. Catalyst regeneration

The spent catalyst was recovered from the reaction mixture by filtration and washed thoroughly with distilled water and dried at 70 °C for reuse.

3. Results and discussion

3.1. Physiochemical characterisation of Co-exchanged zeolites

Fig. 1 displays the DRS spectra of three Co-exchanged zeolites. For the three samples, the spectral minima appear around 530 nm in the visible region and 240 nm in the UV region. These absorptions are assigned to the transition of the octahedral $[Co(H_2O)_6]^{2+}$ complex formed due to the octahedral coordination of the exchanged cobalt ions located in the centre of the zeolite's sodalite cage with 6 water molecules. This complex is also responsible for the hydrolysis and dissolution of zeolites especially at low Si/Al ratio. Additionally,

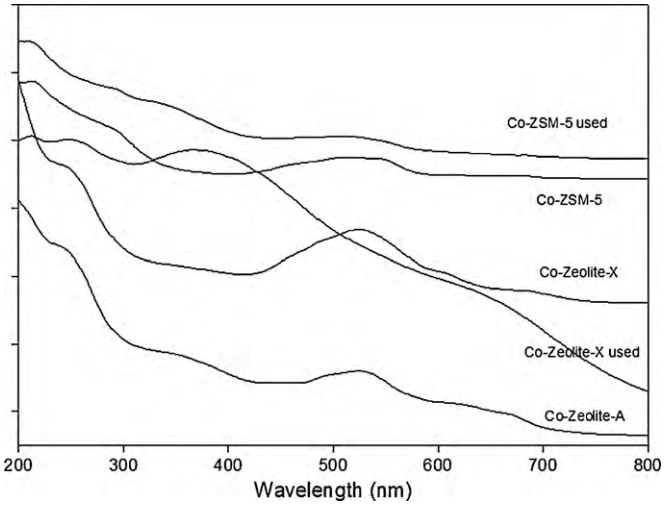

Fig. 1. UV–vis DRS spectra of Co-zeolite before and after reaction.

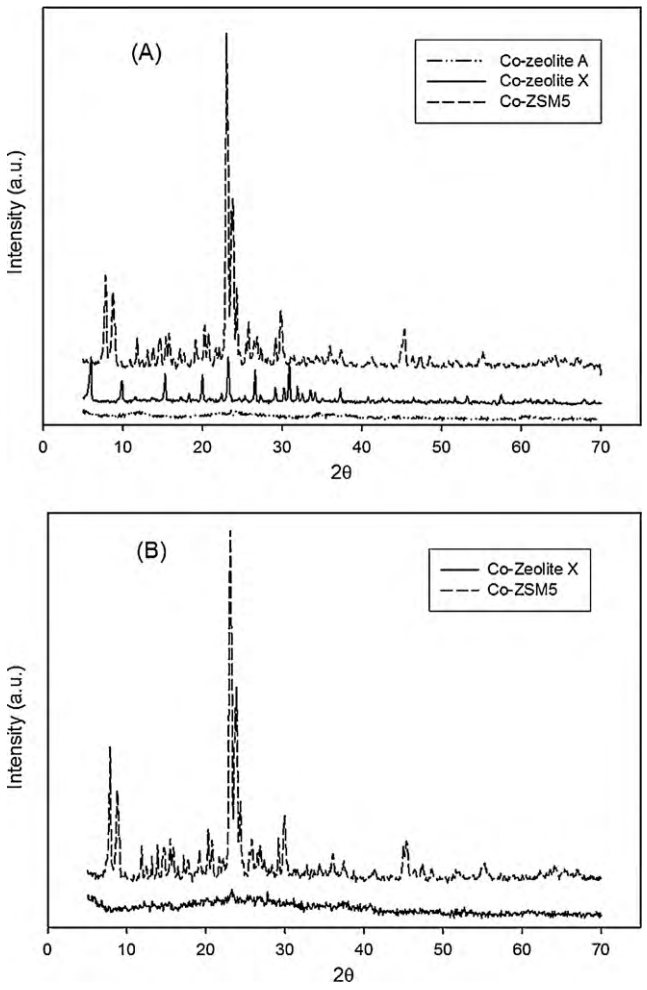

Fig. 2. XRD patterns of Co-exchanged zeolites before and after reaction. (A) Co-zeolite before reaction and (B) Co-zeolite after reaction.

for zeolite-A, a small peak observed at 640 nm is attributed to the cobalt ions present in unit cell body, which confers to the tetragonal coordination with the framework oxygen.

Fig. 2 shows the XRD patterns of the cobalt exchanged zeolite samples. It is observed that Co-ZSM-5 maintains the crystalline structure of ZSM-5, without any changes in the position and intensity of the major diffraction peaks. Co-zeolite-X still keeps the major crystal structure but the intensities of its major peaks are reduced, suggesting a partial loss of its crystallinity and transformation to an amorphous phase, whereas the diffraction peaks for Co-zeolite-A are disappeared suggesting the complete loss of crystallinity. Table 1 shows the crystallinity of the zeolite before and after ion exchange. The crystallinity of the respective Na-zeolite was taken as a reference with its crystallinity as 100%. As shown that the loss of crystallinity for Co-ZSM-5, zeolite-X and zeolite-A is about 17, 83 and 100%, respectively.

Table 1
Crystallinity of Na- and Co-exchanged zeolites.

	% crystallinity of Na form (reference)	% crystallinity after Co ion exchange	% crystallinity of Co-zeolite after reaction
Zeolite-A	100	Amorphous	Sample dissolved
Zeolite-X	100	17.04	Amorphous
ZSM-5	100	83.80	39.86

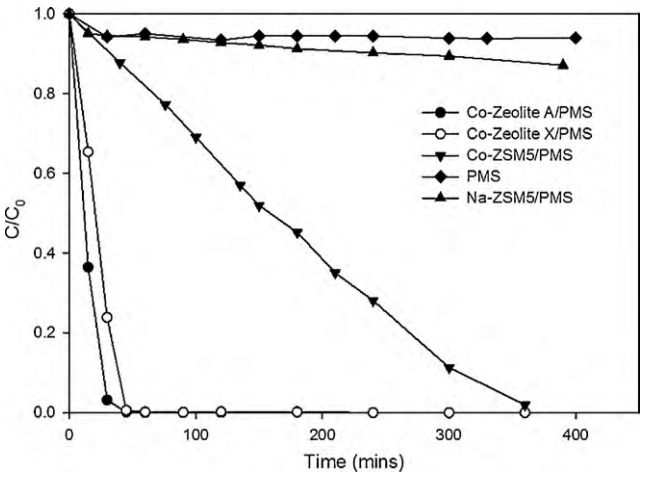

Fig. 3. Phenol degradation kinetics using different cobalt exchanged zeolites [0.4 g/L catalyst, 2 g/L PMS, 25 ppm phenol and 25 °C].

The structural damage of zeolite after cobalt exchange is attributed to the excessive formation of the hydronium ions. It has been reported that the hydrated Co^{2+} is acidic and will result in the formation of H_3O^+ ion and $CoOH^+$ in the exchange solution, which are capable of being exchanged with Na^+ ion in the crystal along with the Co^{2+} ions. This hydronium ion tends to attack the zeolite framework causing the dissolution of the Al^{3+} ions thereby breaking down the unit cell structure [20].

Although the structures of zeolites A and X were considerably lost, the SEM images show a little change in the particle morphology. Both Na- and Co-exchanged zeolite-A and -X samples show rectangular shaped particles with sharp edges at the particle size of 0.5–1 μm. A similar observation for a complete loss of crystallinity and collapse of crystal structure of zeolite-A due to acid consumption, but without any change in the morphology, was also reported earlier [23].

3.2. Catalytic activity and structural stability of Co-zeolite

Preliminary experiments of phenol oxidation were carried out to test Co-zeolite efficiency and stability. Fig. 3 shows the degradation profiles of phenol in the presence of PMS and Co-zeolite catalysts. A control test with only PMS in a homogeneous system shows no significant change in phenol concentration, suggesting no sulphate radical formation and phenol oxidation occurred without Co catalyst. Another control experiment of phenol oxidation in the presence of Na-ZSM-5 with peroxymonosulphate also reveals a much low rate of phenol oxidation, suggesting that Na-ZSM-5 cannot effectively activate peroxymonosulphate to generate sulphate radical for phenol degradation. However, it is observed that the rate of phenol oxidation with Co-zeolite-A/PMS and Co-zeolite-X/PMS is extremely fast with phenol degradation getting completed in less than 30 min whereas it takes around 6 h for complete phenol degradation in the presence of Co-ZSM-5 and PMS. The extremely fast rate of oxidation observed in the presence of Co-zeolite-A and -X is possibly due to the homogeneous reaction between PMS and cobalt ions which are leached into the solution resulted from the collapse and dissolution of the zeolites. This phenomenon was visibly evident in the case of zeolite-A, as the catalyst shows strong dissolution in the solution and recycling of the catalyst by filtration yielded negligible recovery. Zeolite-A is known to consume acid (H^+) ions via hydrolysis and proton ion exchange at acidic pH. During the oxidation reaction, the pH of the solution was around 3–3.5. It is suggested that, the acid consumption of zeolite-A is significantly higher at low pH, which is attributed to the increase of aluminium oxidation state to +3, thereby causing collapse of the structure and dissolution of zeolite-A [23]. Similar to zeolite-A, zeolite-X also gave a very fast reaction suggesting the major leaching of cobalt ion due to structural loss and dissolution. However, unlike Co-zeolite-A, only partial dissolution was observed in Co-zeolite-X and partial recovery of the catalyst was achieved by filtering the solution after the reaction. Fig. 2 shows the XRD profiles of Co-zeolites after reaction and it is seen that Co-zeolite-X exhibits complete loss of crystallinity. However, Co-ZSM-5 can still maintain its crystal structure.

Additionally, the UV–vis DRS spectra (Fig. 1) show no peak of the octahedral $[Co(H_2O)_6]^{2+}$ complex in the post-reaction catalyst of Co-zeolite-X. For Co-ZSM-5, the UV–vis DRS spectrum of post-reaction is almost the same as the one before reaction, but with a slight decrease in the peak intensity of the octahedral complex. Among the three types of catalyst, Co-ZSM-5 shows comparative stable structure and catalytic property. The XRD spectra of the recovered Co-ZSM-5 sample show 40% loss of crystallinity.

It has been proposed that the cobalt exchanged species into ZSM-5 is present in three different forms depending on the Si/Al ratio of the zeolite [22]. The zeolite with a lower Si/Al ratio generally contains the Co^{2+} ions present as an exchangeable ion. These ions are highly active for reaction with peroxymonosulphate, however, during the reaction it gets to a higher oxidation state probably causing the deterioration of the structure and getting leached out, as observed in the case of zeolite-A and -X. Apart from Co^{2+} ions, Co-ZSM-5 also contains the cobalt in the oxide form (generally as Co_3O_4, $CoAl_2O_4$ or CoO). These oxides of Co are much more stable while reacting with peroxymosulphate due to quick oxidation–reduction as per following reaction:

$$HSO_5^- \xrightarrow{Co^{2+}\rightarrow Co^{3+}} SO_4^{\bullet -} + OH^- \quad (5)$$

$$HSO_5^- \xrightarrow{Co^{3+}\rightarrow Co^{2+}} SO_5^{\bullet -} + H^+ \quad (6)$$

Thereby, it allows the Co-ZSM-5 based catalyst to remain partially stable for multiple usages. The amount of cobalt present as exchangeable ion or as an oxide depends significantly on the Si/Al ratio. The Co-ZSM-5 having Si/Al = 15 contains the cobalt mostly in the exchangeable form as Co^{2+} whereas the Co-ZSM-5 having Si/Al = 40 contains the cobalt mostly in the oxide form [24]. In the present case the Si/Al ratio of the ZSM-5 was 25. Roughly assuming a linear co-relation, it can be approximated that almost 50% of the cobalt was present in the ionic form and remaining as an oxide form. Thus the 40% loss in crystallinity of the Co-ZSM-5 after reaction also implies towards the damage of the crystalline structure due to the exchangeable cation whereas the remaining cobalt ions in the oxide form tends to remain in the structure. Based on the observation, it can be proposed that the stability of the Co-ZSM-5 for the reaction would be better for higher Si/Al ratio, as it would have the majority of cobalt in the oxide form.

3.3. Catalytic activity of Co-ZSM-5 with different oxidants

Fig. 4 shows the dynamic variation of phenol concentration under various reaction conditions using ZSM-5 based materials. A control experiment with only Co-exchanged ZSM-5 shows a negligible change in phenol concentration, suggesting a minimal adsorption of phenol on the Co-ZSM-5. However, Co-ZSM-5 with peroxymonosulphate resulted in complete degradation of phenol in less than 6 h. Co-ZSM-5 with other two oxidants, H_2O_2 and persulphate, would only give less than 10% phenol degradation in 6 h, indicating that Co-ZSM-5 could not effectively activate H_2O_2 and persulphate to produce hydroxyl and sulphate radicals, respectively. Anipsitakis and Dionysiou [25] have reported an observation of slow reaction rate for Co^{2+}/H_2O_2 and Co^{2+}/persulphate in homo-

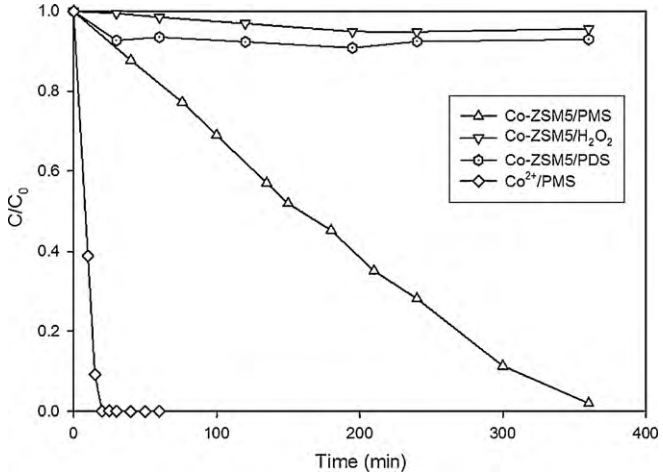

Fig. 4. Preliminary study of phenol degradation using Co-ZSM-5 [0.4 g/L catalyst, 2 g/L PMS, 25 ppm phenol and 25 °C].

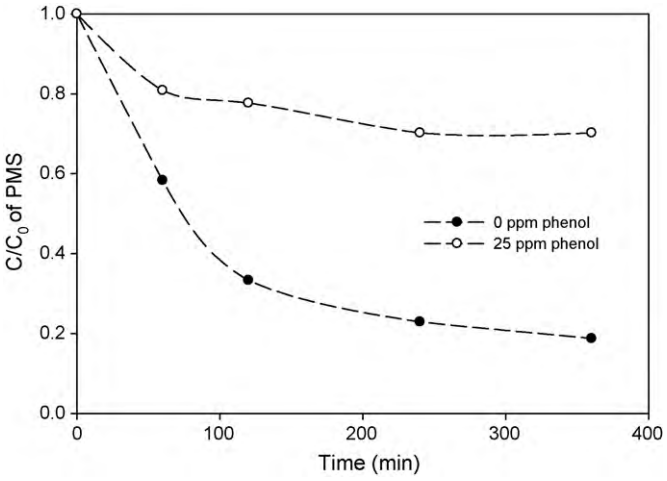

Fig. 6. PMS consumption in the presence and absence of phenol.

geneous systems. Thus, it would be expected a slower reaction rate for heterogeneous systems in this investigation.

3.4. The kinetics of phenol degradation

Fig. 5 shows phenol degradation profiles at varying initial concentrations. It is seen that phenol degradation efficiency changes with its initial concentration. At 12.5 ppm, phenol degradation is very fast and achieves 100% degradation within 4 h, whereas at 50 ppm, the degradation rate is slower and will achieve only 60% degradation within 6 h. It is noted that the rate of phenol degradation rate seems to remain constant throughout the reaction period, resulting in a linear degradation rate profile at each concentration.

The change in TOC was found at 40% removal of organic carbon in the time period of 6 h for the initial phenol concentration of 25 ppm, suggesting that majority of the degradation products still remain in water. However, a few runs were carried out overnight and the TOC measurement showed more than 75% removal. The extent of TOC removal varies with the initial concentration with the highest TOC removal observed for the lowest initial concentration of phenol. This is mostly due to the fact that upon complete removal of phenol, the generated active radical tends to react with the intermediate causing higher TOC reduction.

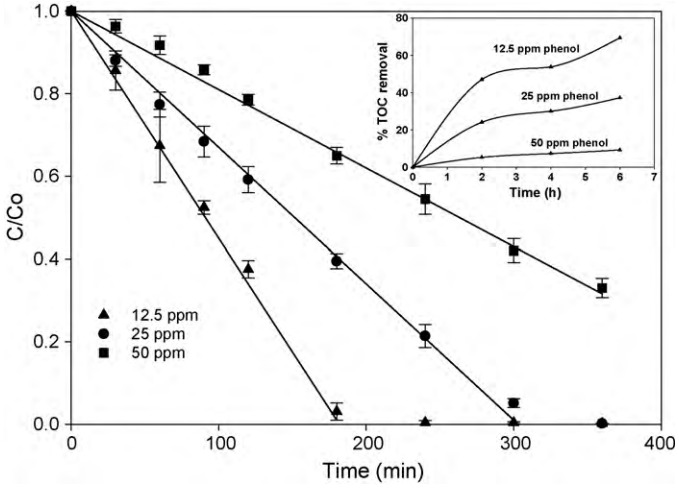

Fig. 5. Phenol degradation kinetics at different initial concentrations of phenol [0.4 g/L catalyst, 2 g/L PMS, and 25 °C].

An interesting observation was made in regards to the change in PMS concentration. As observed in Fig. 6, PMS concentration is much less in the solution without phenol, suggesting the fast reaction of PMS with Co-ZSM-5. In the absence of phenolic contaminant in the solution, PMS exhibits 80% conversion while only 25% PMS was consumed during the reaction having 25 ppm of phenol. This is probably due to the self-consumption of PMS by the generated sulphate radical. The low conversion of PMS may also be the reason for low TOC removal during the 6 h and further oxidation for high TOC removal in a longer time.

The oxidation of a phenolic pollutant can either take place on the surface of catalyst after the adsorption of phenol molecules on Co-ZSM-5 or in the solution after the desorption of the generated active sulphate radical from the catalyst surface. The linear rate of phenol removal from the solution infers that the limiting step of phenol degradation is the generation of sulphate radical on the catalyst surface. Fernandez et al. [26] proposed the kinetic rate equation as per the following Eq. (7):

$$\frac{dC_{ph}}{dt} = k_{Co}[Co^{2+}] \tag{7}$$

In the current experiment of phenol degradation for a fixed amount of cobalt catalyst and assuming a zero-order kinetics of phenol removal, the mass balance on the batch reactor can be written as Eq. (8):

$$V\frac{dC_{Ph}}{dt} = -(r_{Ph})W = -k_{Co}W \tag{8}$$

where C_{ph} is the phenol concentration at any instant time 't', k_{Co} is the apparent zero order rate constant, W is the mass of the catalyst and V is the volume of the reactor. Integration of the above equation results in the mathematical model of the degradation profile. The rate constant at varying phenol concentration is depicted in Table 2. As seen, rate constant will decrease as the concentration increases.

Table 2
Rate constant at different feed concentrations of phenol.

Initial phenol concentration	Rate constant × 10^{-4} (min^{-1})
12.5 ppm	1.25
25 ppm	0.75
50 ppm	0.25

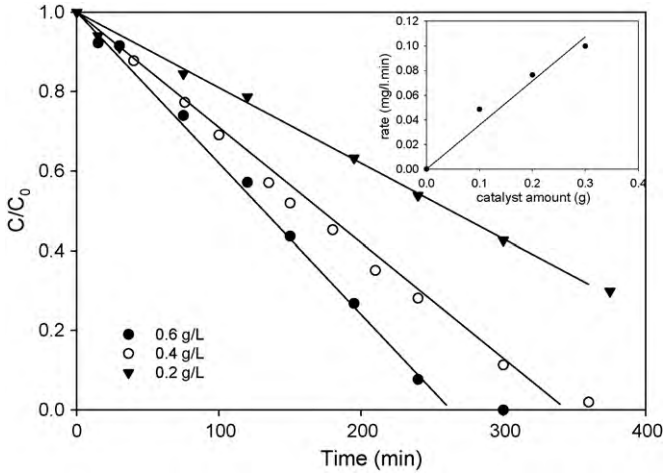

Fig. 7. Effect of catalyst amount on the reaction rate [2 g/L PMS, 25 ppm phenol and 25 °C].

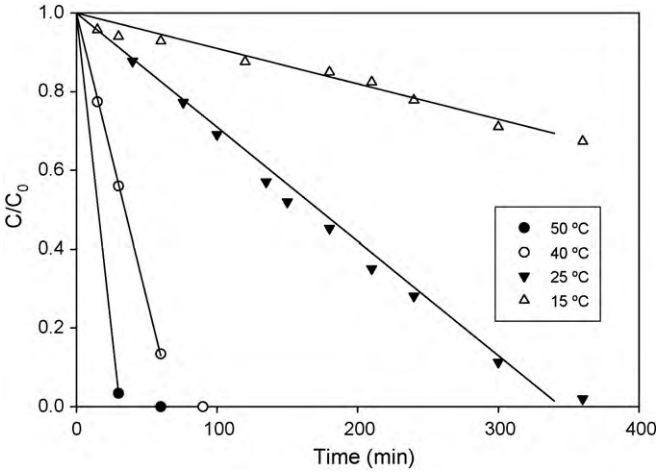

Fig. 9. Temperature effect on the degradation rate of phenol with Co-ZSM-5 [0.4 g/L catalyst, 2 g/L PMS, 25 ppm phenol].

3.5. Effect of reaction parameters on phenol degradation kinetics

3.5.1. Effect of catalyst and oxidant amount

The dynamic degradation of phenol at different Co-ZSM-5 loading in solution is shown in Fig. 7 along with the rate constant profile in the insert figure. As seen, the rate of phenol degradation increases with the increase in catalyst loading from 0.2 to 0.6 g/L. The plot of rate constant with respect to catalyst amount results in a straight line thereby implying that the reaction rate constant is the first order with respect to the concentration of catalyst. It can be noted from the kinetic Eq. (8) that the rate of phenol degradation is linearly dependent on the cobalt concentration. As the amount of catalyst in the solution is increased, the extent of active sites having cobalt ion increases thereby resulting in an enhancement in generation of sulphate radical, which in turn increases the rate of oxidation.

Fig. 8 shows the effect of peroxymonosulphate concentration on phenol degradation. As observed in the insert figure, the rate of phenol oxidation was slightly improved by increasing PMS concentration and a plateau was reached after 1 g PMS in solution. Further increase in PMS loading will not result in significant improvement in the rate of reaction. This is justified that a fixed amount of catalyst puts an upper limit on the rate of generation of sulphate radical.

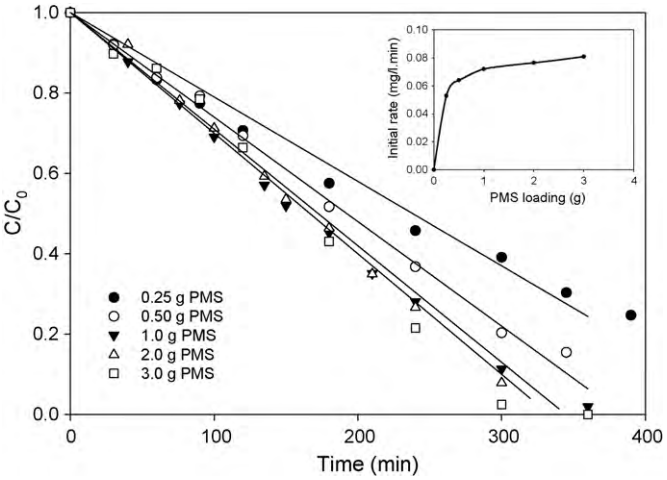

Fig. 8. Phenol degradation at different amounts of PMS [0.4 g/L catalyst, 25 ppm phenol and 25 °C].

Since the peroxymonosulphate is inactive by itself, the presence of excess oxidant has no influence (Fig. 3).

3.5.2. Effect of reaction temperature

The temperature significantly affects the rate of reaction and the reaction rate constant generally follows the Arrhenius correlation. Fig. 9 displays the variation of phenol concentration at varying temperatures. From the figure, it is seen that phenol degradation is quite low at low temperature and will increase significantly with increasing temperature. At 15 °C, phenol degradation efficiency was only 30% in 6 h, while it reached to 100% in 90 and 60 min, respectively, at temperatures of 40 and 50 °C. Based on zero-order kinetics, the relationship between phenol degradation rate and temperature was found to follow the Arrhenius equation and the activation energy was obtained as 69.7 kJ/mol.

3.6. Reaction quenching studies

Activation of PMS with cobalt tends to generate two major kinds of radical, *viz.* hydroxyl radical and sulphate radical. A small amount of peroxymonosulphate radical ($SO_5^{\bullet -}$) is generated simultaneously [27], however its activity is too low to be considered for taking part in the oxidation reaction. In order to classify the type of active radicals present in the reaction system and their role, a few quenching tests were carried out to check the active radicals. Two different types of alcohols, *viz.* ethanol and tertiary butanol were used as quenching reagents with different concentrations. Ethanol is capable of quenching both sulphate and hydroxyl radicals as it has a high reactivity towards both radicals, whereas tertiary butanol mainly reacts with hydroxyl radical and much slowly with sulphate radical [28].

Fig. 10 shows the rate of phenol oxidation under the influence of both quenching reagents. It is observed that the rate of reaction is negligibly affected at lower concentration of ethanol (0.75 ml) despite the fact that ethanol is a strong quencher of both the sulphate and peroxide radicals. On further increase in the concentration of ethanol to 7.5 ml, the rate of phenol oxidation was found to decrease significantly, showing only 50% oxidation in the reaction period of 6 h. The reaction carried out under the similar concentration of tertiary butanol shows a very slight reduction in the rate of phenol oxidation. Further increase in the concentration of tertiary butanol in solution, phenol degradation would be similar, thereby suggesting that the major radical formed in the given reaction is sulphate, however, a presence of small quantity of hydroxyl

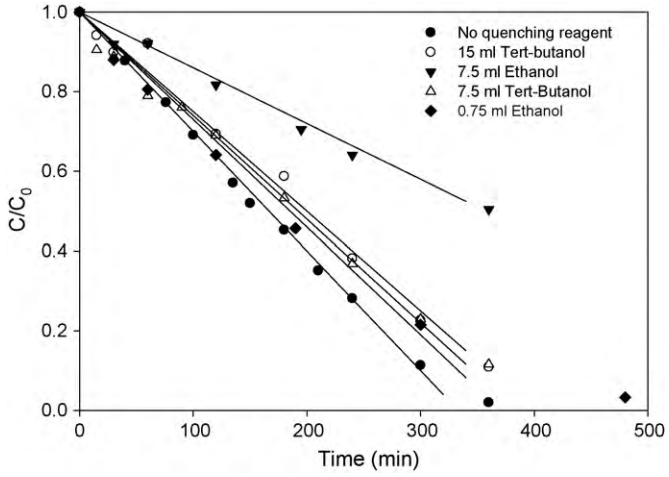

Fig. 10. Reaction quenching of phenol oxidation with Co-ZMS-5 in the presence of ethanol and tert-butanol [0.4 g/L catalyst, 2 g/L PMS, 25 ppm phenol and 25 °C].

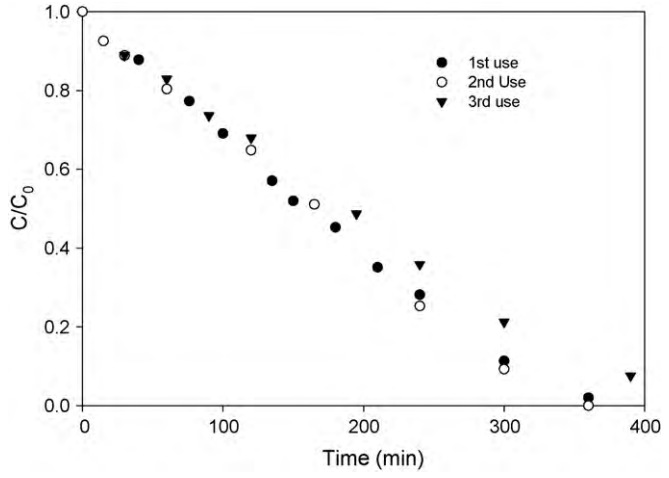

Fig. 11. Phenol degradation in the tests of recycled Co-ZSM-5 [0.4 g/L catalyst, 2 g/L PMS, 25 ppm phenol and 25 °C].

radical cannot be ruled out due to the slight reduction in the rate of phenol on addition of tertiary butanol.

3.7. Reactivity of spent Co-ZSM-5 catalyst and reusability

Fig. 11 shows the catalytic activity of recycled Co-ZSM-5 for phenol degradation. As seen, the catalyst activity remained unaffected in the second round reuse and decreased slightly in the third test. The analysis of the solution using AAS shows a negligible presence of Co ion in the second test and 0.2 ppm Co ion leaching in the third recycled test. This suggests that the cobalt ion was bonded strongly in ZSM-5 framework, making it quite stable performance in the reaction.

4. Conclusions

Co ion-exchanged zeolites are effective catalysts for phenol oxidative degradation using peroxymonosulphate but they are not active for phenol oxidation using H_2O_2 and persulphate. Zeolite-A and zeolite-X after Co ion exchange lose the crystallinity and show strong leaching of Co ion in solution, resulting in much faster reaction rate for homogeneous activation of peroxymonosulphate. ZSM-5 exhibits stable crystalline structure after Co ion exchange and presents stable performance in heterogeneous phenol oxidation in several runs. The phenol degradation follows zero-order kinetics with the activation energy of 69.7 kJ/mol. Several operation parameters affect the phenol oxidation. The loading of Co-ZSM-5 shows a linear relationship with reaction rate while the PMS concentration shows less effect on reaction rate. Co-ZSM-5 can be used for multiple catalytic tests.

References

[1] R. Andreozzi, V. Caprio, A. Insola, R. Marotta, Catalysis Today 53 (1999) 51–59.
[2] S. Wang, Dyes and Pigments 76 (2008) 714–720.
[3] Y. Wang, C.-S. Hong, Water Research 33 (1999) 2031–2036.
[4] Q. Yang, H. Choi, D.D. Dionysiou, Applied Catalysis B: Environmental 74 (2007) 170–178.
[5] T.E. Agustina, H.M. Ang, V.K. Vareek, Journal of Photochemistry & Photobiology, C: Photochemistry Reviews 6 (2005) 264–273.
[6] G.P. Anipsitakis, D.D. Dionysiou, Environmental Science & Technology 37 (2003) 4790–4797.
[7] X. Chen, X. Qiao, D. Wang, J. Lin, J. Chen, Chemosphere 67 (2007) 802–808.
[8] J. Madhavan, P. Maruthamuthu, S. Murugesan, S. Anandan, Applied Catalysis B: Environmental 83 (2008) 8–14.
[9] Z.Y. Yu, L. Kiwi-Minsker, A. Renken, J. Kiwi, Journal of Molecular Catalysis A: Chemical 252 (2006) 113–119.
[10] P.R. Shukla, S.B. Wang, H.M. Ang, M.O. Tade, Separation and Purification Technology 70 (2010) 338–344.
[11] D. Lison, CRC Critical Reviews in Toxicology 26 (1996) 585–616.
[12] G. Anipsitakis, E. Stathatos, D. Dionysiou, Journal of Physical Chemistry B 109 (2005) 13052–13055.
[13] Q. Yang, H. Choi, Y. Chen, D.D. Dionysiou, Applied Catalysis B: Environmental 77 (2008) 300–307.
[14] L.B. Pierella, C. Saux, S.C. Caglieri, H.R. Bertorello, P.G. Bercoff, Applied Catalysis A: General 347 (2008) 55–61.
[15] M. Dry, Applied Catalysis A: General 276 (2004) 1–3.
[16] J. Sebastian, K. Jinka, R. Jasra, Journal of Catalysis 244 (2006) 208–218.
[17] J. Sebastian, R. Jasra, Industrial & Engineering Chemistry Research 44 (2005) 8014–8024.
[18] L.B. Pierella, C. Saux, H.R. Bertorello, P.G. Bercoff, P.M. Botta, J. Rivas, Materials Research Bulletin 43 (2008) 2026–2035.
[19] A.A. Verberckmoes, B.M. Weckhuysen, R.A. Schoonheydt, Microporous and Mesoporous Materials 22 (1998) 165–178.
[20] P.E. Riley, K. Seff, The Journal of Physical Chemistry 79 (1975) 1594–1601.
[21] D. Bae, K. Seff, Microporous and Mesoporous Materials 33 (1999) 265–280.
[22] K. Góra-Marek, B. Gil, M. Sliwa, J. Datka, Applied Catalysis A: General 330 (2007) 33–42.
[23] T. Cook, W. Cilley, A. Savitsky, B. Wiers, Environmental Science & Technology 16 (1982) 344–350.
[24] K. Góra-Marek, J. Datka, Catalysis Today 137 (2008) 466–470.
[25] G.P. Anipsitakis, D.D. Dionysiou, Environmental Science & Technology 38 (2004) 3705–3712.
[26] J. Fernandez, P. Maruthamuthu, A. Renken, J. Kiwi, Applied Catalysis B: Environmental 49 (2004) 207–215.
[27] G. McLachlan, J. Muller, S. Rokita, C. Burrows, Inorganica Chimica Acta 251 (1996) 193–199.
[28] R. Jameton, J. Muller, C. Burrows, Comptes Rendus-Chimie 5 (2002) 461–466.